Exclusive Vector Meson Production and Deeply Virtual Compton Scattering at HERA

Alessia Bruni[1], *Xavier Janssen*[2], *Pierre Marage*[2]
[1] Istituto Nazionale di Fisica Nucleare, Via Irnerio 46, I-40126 Bologna, Italy
[2] Faculty of Science, Université Libre de Bruxelles, Bd. du Triomphe, B-1040 Brussels, Belgium

Abstract
Exclusive vector meson production and deeply virtual Compton scattering are ideally suited reactions for studying the structure of the proton and the transition from soft to hard processes. The main experimental data obtained at HERA are summarised and presented in the light of QCD approaches.

1 Introduction

The two processes which are the object of the present report, the exclusive production of a vector meson (VM) of mass M_V, $e+p \to e+VM+Y$, and deeply virtual Compton scattering (DVCS), $e+p \to e+\gamma+Y$, where Y is a proton (elastic scattering) or a diffractively excited system (proton dissociation), are characterised in Fig. 1. The kinematical variables are Q^2, the negative square of the photon four-momentum, W the photon-proton centre of mass energy ($W^2 \simeq Q^2\,(1/x-1)$, x being the Bjorken scaling variable) and t, the square of the four-momentum transfer at the proton vertex.

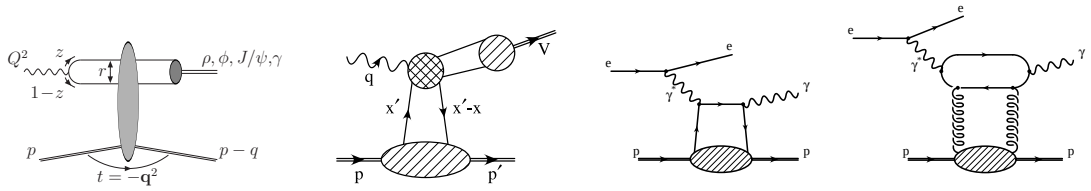

Fig. 1: (from left to right) Representative diagrams of a) low x dipole approach and b) GPD approach, for VM production; c) LO scattering and d) two gluon exchange, for the DVCS process.

The H1 and ZEUS collaborations at HERA have studied the elastic and proton dissociative production of ρ [1–4], ω [5], ϕ [3,6], J/ψ [7,8], $\psi(2s)$ [9] and Υ [10,11] mesons, and the DVCS process in the elastic channel [12, 13]. The measurements are performed in the low x, large W domain $10^{-4} \lesssim x \lesssim 10^{-2}$, $30 \leq W \leq 300$ GeV. They cover photoproduction ($Q^2 \simeq 0$), with $|t|$ values up to 30 GeV^2, and electroproduction in the deep inelastic (DIS) domain ($2 \leq Q^2 \leq 90\ \mathrm{GeV}^2$) with $|t| \lesssim 2\ \mathrm{GeV}^2$. The cross sections, expressed in terms of $\gamma^* p$ scattering, are measured differentially in Q^2, W and t. The measurement of angular distributions gives access to spin density matrix elements and polarised amplitudes.

1.1 Production mechanisms

Within the QCD formalism, two main complementary approaches are used to describe VM production and DVCS: dipole factorisation and collinear factorisation.

Dipole approach of VM production At high energy, i.e. small x, VM production can be described in the proton rest frame with three factorising contributions [14] (see Fig. 1a): the fluctuation of the virtual photon into a $q\bar{q}$ colour dipole, the elastic or proton dissociative dipole–proton scattering, and the $q\bar{q}$ recombination into the final state VM. The dipole–proton cross section is expected to be flavour independent and governed by the transverse size of the dipole. Light VM photoproduction is dominated by large dipoles, leading to large interaction cross sections with the incoming proton, similar to soft hadron–hadron interactions. In contrast, heavy VM production and large Q^2 processes are dominated by small dipoles, with smaller cross sections implied in QCD by colour transparency, the quark and the antiquark separated by a small distance tending to screen each other's colour.

The cross section for VM production can be computed at small x and for all Q^2 values through models [15–17] using universal dipole–proton cross sections measured in inclusive processes, possibly including saturation effects [18] (see also [19]). This formalism thus connects the inclusive and diffractive cross sections, also in the absence of a hard scale.

In the presence of a hard scale (large quark mass or Q), the dipole–proton scattering is modelled in perturbative QCD (pQCD) as the exchange of a colour singlet system consisting of a gluon pair (at lowest order) or a BFKL ladder (at leading logarithm approximation, LL $1/x$). At these approximations, the cross sections are proportional to the square of the gluon density $|xG(x)|^2$ in the proton [20]. The pQCD calculations [21–24] use k_t-unintegrated gluon distributions (see also [25]). The typical interaction scale is $\mu^2 \simeq z(1-z)(Q^2+M_V^2)$, where z is the fraction of the photon longitudinal momentum carried by the quark. For heavy VM (in the non-relativistic wave function (WF) approximation) and for light VM production from longitudinally polarised photons, $z \simeq 1/2$ and the cross sections are expected to scale with the variable $\mu^2 = (Q^2+M_V^2)/4$. In contrast, for light VM production by transversely polarised photons, contributions with $z \to 0,1$ result in the presence of large dipoles and the damping of the scale μ, thus introducing non-perturbative features even for non-small Q^2.

Collinear factorisation and GPD In a complementary approach (see Fig. 1b), a collinear factorisation theorem [26] has been proven in QCD for longitudinal amplitudes in the DIS domain, which does not require low x values. This allows separating contributions from different scales, a large scale at the photon vertex, provided by the photon virtuality Q (or the quark mass), and a small scale for the proton structure. The latter is described by Generalised Parton Distributions (GPD – see e.g. the reviews [27]), which take into account the distribution of transverse momenta of partons with respect to the proton direction and longitudinal momentum correlations between partons. They account for "off-diagonal" or "skewing" effects arising from the kinematic matching between the initial state (virtual) photon and the final state, VM or real photon for DVCS. GPD calculations have been performed for light VM electroproduction [28]. NLO corrections to light VM electroproduction and to heavy VM photoproduction have been computed [29].

DVCS Following collinear factorisation, the DVCS process is described at LO by Fig. 1c, where the virtual photon couples directly to a quark in the proton. QCD calculations at the scale $\mu^2 = Q^2$ involve GPD distributions [30, 31]. At higher order, two gluon exchange as in Fig. 1d gives also an important contribution at HERA. Joint fits to DVCS and inclusive structure functions data have been used to extract GPD distributions [32].

Large $|t|$ production Calculations for VM production at large $|t|$ have been performed both in a DGLAP and in a BFKL approach (see section 6).

1.2 Measurements at HERA

Vector mesons are identified by H1 and ZEUS via their decay to two oppositely charged particles $\rho \to \pi^+\pi^-$, $\phi \to K^+K^-$, $J/\psi \to e^+e^-, \mu^+\mu^-$ and $\Upsilon \to \mu^+\mu^-$. The kinematic variables are reconstructed from the scattered electron and decay particle measurements. Forward calorimeters and taggers at small angles are generally used to separate elastic and proton dissociative events. The scattered proton is also measured in forward proton spectrometers, with an acceptance of a few %, allowing the selection of a purely elastic sample and the direct measurement of the t variable.

VM production has been investigated mainly using the HERA I data, collected between 1992 and 2000 and corresponding to an integrated luminosity of $\simeq 150$ pb^{-1} for both collaborations. The integrated luminosity of 500 pb^{-1} collected at HERA II (2003-2007) has been analysed so far for DVCS [13] and Υ [11]. For HERA II, ZEUS has installed a microvertex detector but has removed the small angle detectors: the leading proton spectrometer and the forward and rear calorimeters, compromising the precise analysis of diffractive data. The HERA II analyses of H1 will benefit of the fast track trigger installed in 2002 and, for general diffraction studies, of the very forward proton spectrometer VFPS installed in 2003, which however has very limited acceptance for VM.

2 From soft to hard diffraction: t dependences and the size of the interaction

The t dependences of DVCS and VM production provide information on the size and the dynamics of the processes and on the scales relevant for the dominance of perturbative, hard effects. Whereas total cross sections (F_2 measurements) are related, through the optical theorem, to the scattering amplitudes in the forward direction, diffractive final states provide a unique opportunity to study the region of non-zero momentum transfer t. This gives indirect information on the variable conjugate to t, the transverse size of the interaction.

For $|t| \lesssim 1-2$ GeV^2, the $|t|$ distributions are exponentially falling with slopes b: $\mathrm{d}\sigma/\mathrm{dt} \propto \mathrm{e}^{-\mathrm{b}|\mathrm{t}|}$. In an optical model approach, the diffractive b slope is given by the convolution of the transverse sizes of the interacting objects: $b = b_{q\bar{q}} + b_Y + b_{I\!P}$, with contributions of the $q\bar{q}$ dipole, of the diffractively scattered system (the proton or the excited system Y) and of the exchange ("Pomeron") system. Neglecting effects related to differences in the WF, universal b slopes are thus expected for all VM with the same $q\bar{q}$ dipole sizes, i.e. with the same values of the scale $\mu^2 = (Q^2 + M_V^2)/4$. Conversely, elastic and proton dissociative slopes are expected to differ for all VM production at the same scale by the same amount, $b_p - b_Y$. Measurements of elastic and

proton dissociative b slopes for DVCS and VM production are presented in Fig. 2 as a function of the scale μ [1].

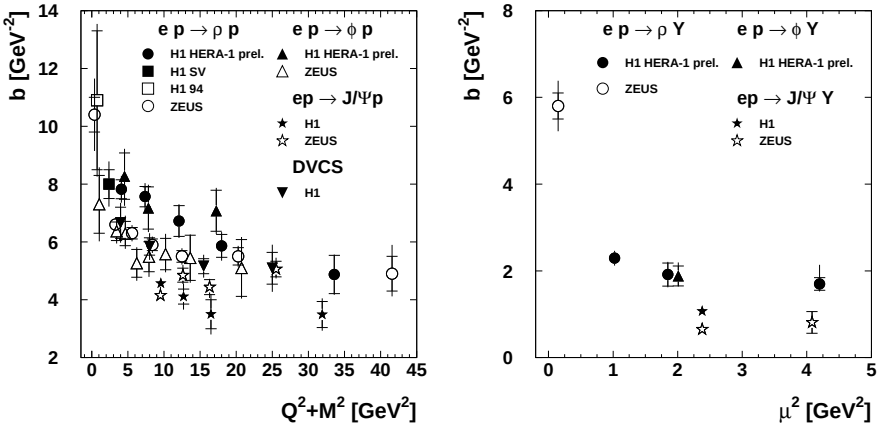

Fig. 2: Measurement of (left) the elastic and (right) the proton dissociative slopes b of the exponential t distributions, as a function of the scale $\mu^2 = (Q^2 + M_V^2)/4$ for VM production and $\mu^2 = Q^2$ for DVCS.

For J/ψ elastic production, the b slope is $\lesssim 4.5$ GeV^{-2}, with no visible Q^2 dependence. This value may be related to the proton form factor [16]. For proton dissociation, the b slope is below 1 GeV^{-2}, putting an upper limit to the transverse size of the exchange (with the assumption that $b_Y \simeq 0$ for proton dissociation).

At variance with J/ψ production, which is understood as a hard process already in photoproduction, a strong decrease of b slopes for increasing values of $\mu^2 = (Q^2 + M_V^2)/4$ is observed for light VM production, both in elastic and proton dissociative scattering. A similar scale dependence is observed for DVCS. This is consistent with a shrinkage of the size of the initial state object with increasing Q^2, i.e. in the VM case a shrinkage of the colour dipole. It should however be noted that, both in elastic and proton dissociative scatterings, b slopes for light VM remain larger than for J/ψ when compared at the same values of the scale $(Q^2 + M_V^2)/4$ up to $\gtrsim 5$ GeV^2. The purely perturbative domain may thus require larger scale values.

3 From soft to hard diffraction: W dependences vs. mass and Q^2

Figure 3-left presents measurements as a function of W of the total photoproduction cross section and of the exclusive photoproduction cross sections of several VM; ρ electroproduction cross sections for several values of Q^2 are shown in Fig. 3-right. As expected for decreasing dipole sizes, the cross sections at fixed values of W decrease significantly with increasing VM mass or Q^2. In

[1] Differences between the H1 and ZEUS measurements for elastic scattering are due to differences in background subtraction. The major effect is due to the subtraction of ρ' production by H1, a contribution evaluated to be negligible by ZEUS. Another difference concerns the values used for the b slopes of the proton dissociative contamination.

addition, different reactions exhibit strongly different W dependences. The total photoproduction cross section and the photoproduction of light VM show weak energy dependences, typical of soft, hadron–hadron processes. In contrast, increasingly steep W dependences are observed with increasing mass or Q^2. In detail, the W dependences are investigated using a parameterisation inspired by Regge theory, in the form of a power law with a linear parameterisation of the effective trajectory

$$\sigma \propto W^{\delta}, \quad \delta = 4\,(\alpha_{I\!P} - 1), \quad \alpha_{I\!P}(t) = \alpha_{I\!P}(0) + \alpha' \cdot t. \tag{1}$$

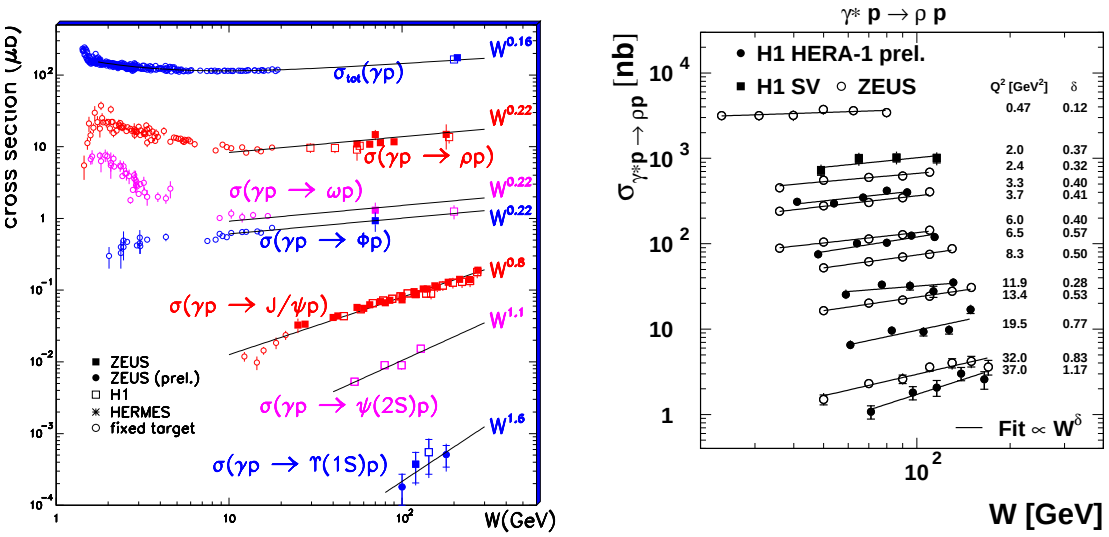

Fig. 3: W dependences of (left) total and VM photoproduction cross sections; (right) ρ electroproduction for several values of Q^2. The lines show fits to the form W^{δ}.

The intercept $\alpha_{I\!P}(0)$ of the effective trajectory quantifies the energy dependence of the reaction for $t = 0$. The evolution of $\alpha_{I\!P}(0)$ with μ^2 is shown in Fig. 4-left. Light VM production at small μ^2 gives values of $\alpha_{I\!P}(0) \lesssim 1.1$, similar to those measured for soft hadron–hadron interactions [33]. In contrast larger values, $\alpha_{I\!P}(0) \gtrsim 1.2$, are observed for DVCS, for light VM at large Q^2 and for heavy VM at all Q^2. This increase is related to the large parton densities in the proton at small x, which are resolved in the presence of a hard scale: the W dependences of the cross section is governed by the hard $x^{-\lambda}$ evolution of the gluon distribution, with $\lambda \simeq 0.2$ for $Q^2 \simeq M^2_{J/\psi}$. The W dependences of VM cross sections, measured for different Q^2 values, are reasonably well described by pQCD models (not shown). In detail these are however sensitive to assumptions on the imput gluon densities in the domain $10^{-4} \lesssim x \lesssim 10^{-2}$ which is poorly constrained by inclusive data [25, 34].

The slope α' in eq. (1) describes the correlation between the t and W dependences of the cross section. The measurement of the evolution with t of the δ exponent can be parameterised as a W dependence of the b slopes, with $b = b_0 + 4\alpha' \ln W/W_0$. In hadron–hadron scattering,

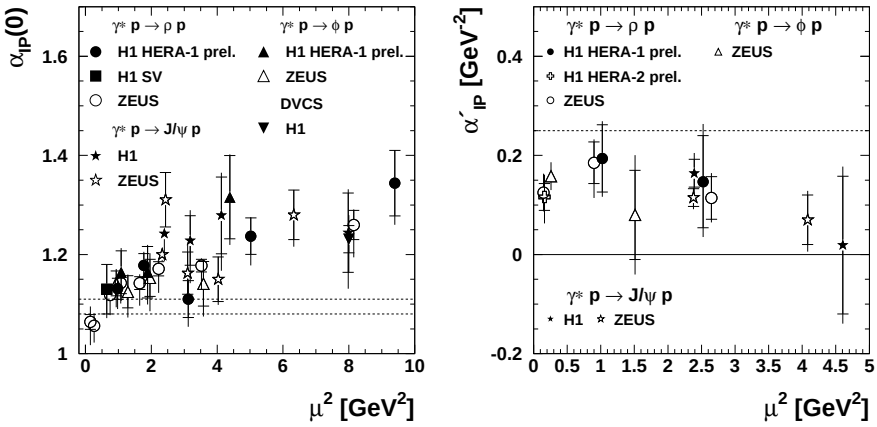

Fig. 4: Values of (left) the intercept $\alpha_{I\!P}(0)$ and (right) the slope α' of the effective Pomeron trajectory, obtained from fits of the W cross section dependences to the form $d\sigma/dt \propto W^{4(\alpha_{I\!P}(0)+\alpha' \cdot t-1)}$. The scales are $\mu^2 = Q^2$ for DVCS and $\mu^2 = (Q^2+M_V^2)/4$ for VM production. The dotted lines represent typical values for hadron–hadron scattering.

positive values of α' are measured, with $\alpha' \simeq 0.25\ \mathrm{GeV}^{-2}$ [35]. This shrinkage of the diffractive peak indicates the expansion with energy of the size of the interacting system, i.e. the expansion of the gluon cloud in the periphery of the interaction. HERA measurements are presented in Fig. 4-right. The values of α' are positive and appear smaller than in hadron–hadron interactions, also for ρ photoproduction. This suggests a limited expansion of the systems considered here on the relevant interaction time scale. In a BFKL approach, α' is related to the average k_t of gluons around the ladder in their random walk, and is expected to be small [36].

4 Q^2 dependences in DVCS and VM production

The description of the Q^2 dependences of the cross sections is a challenge, in view of the presence of higher order corrections and of non-perturbative effects, especially for transverse VM production.

4.1 DVCS

The DVCS cross section depends on the proton GPD distributions. To investigate the dynamical effects due to QCD evolution, the Q^2 dependence has been measured and studied [13] as a function of the dimensionless scaled variable S,

$$S = \sqrt{\sigma_{DVCS}\ Q^4\ b(Q^2)\ /\ (1+\rho^2)},$$

which removes the effects of the photon propagator and of the Q^2 dependence of the b slope, and of the ratio R of the imaginary parts of the DVCS and DIS amplitudes,

$$R = \frac{\mathcal{I}mA(\gamma^* p \to \gamma p)_{t=0}}{\mathcal{I}mA(\gamma^* p \to \gamma^* p)_{t=0}} = 4\frac{\sqrt{\pi\ \sigma_{DVCS}\ b(Q^2)}}{\sigma_T(\gamma^* p \to X)}\ \sqrt{1+\rho^2},$$

with $\sigma_T(\gamma^* p \to X) = 4\pi^2 \alpha_{EM} F_T(x,Q^2)/Q^2$, $F_T = F_2 - F_L$ and $\rho = \mathcal{R}eA/\mathcal{I}mA$ determined from dispersion relations [31].

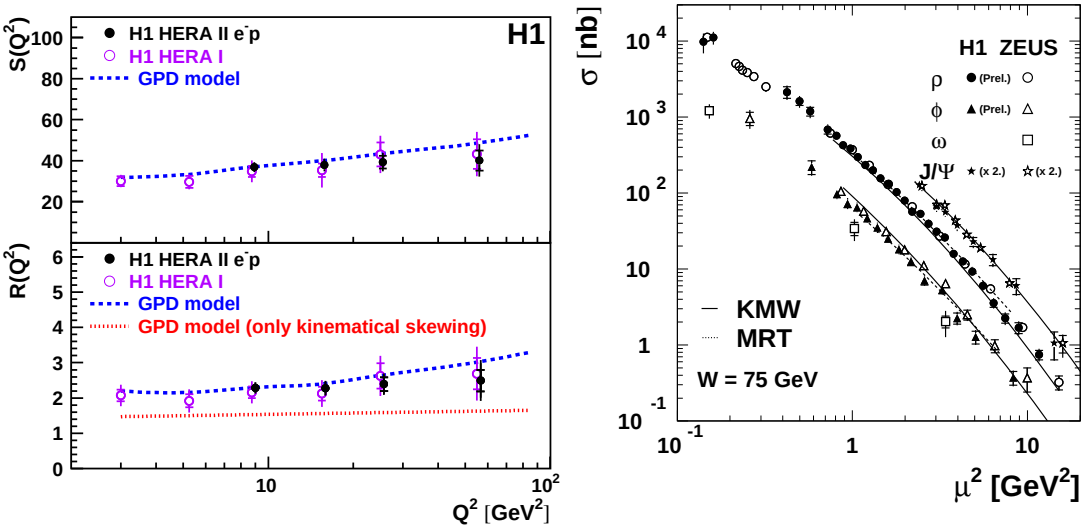

Fig. 5: (left) Q^2 dependences of the observables S and R for DVCS (see text); (right) ρ, ω, ϕ and J/ψ elastic production cross sections, as a function of the scale $\mu^2 = (Q^2 + M_V^2)/4$; for readability of the figure, the J/ψ cross sections have been multiplied by a factor 2. The curves are predictions of the KMW [16] and MRT [23] models.

Figure 5-upper-left shows a weak rise of S with Q^2, which is reasonably well described by the GPD model [30] using the CTEQ PDF parameterisation [37]. The large effect of skewing is visible in Fig. 5-lower-left, where the variable R takes values around 2, instead of 1 in the absence of skewing. GPD calculations [30] compare well with measurements, whereas the same figure shows that it is not sufficient to include only the kinematic contribution to skewing, and that the Q^2 evolution of the GPD must also be taken into account.

4.2 Vector mesons

The elastic production cross sections ρ, ω, ϕ and J/ψ are shown in Fig. 5-right, as a function of the scaling variable $(Q^2 + M_V^2)/4$ (for readability, the J/ψ cross sections have been multiplied by 2) [2]. It is striking that, whereas light VM and J/ψ production cross sections for the same value of Q^2 differ by orders of magnitude (see Fig. 3-left for $Q^2 = 0$), they are close when plotted as a function of the scaling variable $(Q^2 + M_V^2)/4$, up to the factors accounting for the VM charge

[2] Whereas the H1 and ZEUS measurements for ρ agree well, ϕ measurements of ZEUS are a factor 1.20 above H1. When an improved estimation of the proton-dissociation background, investigated for the latest ZEUS ρ production study [2], is used to subtract this background in their ϕ analysis, the cross section ratio of the two experiments is reduced to 1.06, which is within experimental errors.

content ($\rho : \phi : J/\psi = 9 : 2 : 8$) [3]. This supports the dipole approach of VM production at high energy.

The cross sections are roughly described by power laws $1/(Q^2+M_V^2)^n$, with $n \simeq 2.2-2.5$. The simple $n = 3$ dependence expected in a two-gluon approach for the dominant longitudinal cross sections is modified not only by an additional factor $1/Q^2$ in the transverse amplitudes, but also by the Q^2 dependence of the gluon distribution at small x, described by the DGLAP evolution equations. Calculations using the k_t-unintegrated gluon distribution model of MRT [23] or the GPD model [28] (not shown) give reasonable descriptions of the $(Q^2+M_V^2)$ dependences. However, in detail, a good description necessitates the precise modelisation of the Q^2 dependence of the longitudinal to transverse cross section ratio R, with non-perturbative effects affecting σ_T. Dipole models using different saturation and WF parameterisations, e.g. the FSS [15], KMW [16] and DF [17] models, attempt at describing VM production over the full Q^2 range, including photoproduction, with reasonable success.

5 Matrix elements and σ_L/σ_T

Measurements of the VM production and decay angular distributions give access to spin density matrix elements, which are related to the helicity amplitudes $T_{\lambda_V \lambda_\gamma}$ [38]. Analyses of ρ, ϕ and J/ψ photo- and electroproduction indicate the dominance of the two s-channel helicity conserving (SCHC) amplitudes, the transverse T_{11} and the longitudinal T_{00} amplitudes, In the accessible Q^2 ranges, J/ψ production is mostly transverse, whereas for light VM electroproduction the longitudinal amplitude T_{00} dominates (see Fig. 6a and Fig. 7a). In ρ and ϕ electroproduction, a significant contribution of the transverse to longitudinal helicity flip amplitude T_{01} is observed. The amplitude ratio T_{01}/T_{00} decreases with Q^2 (Fig. 6b) and increases with $|t|$ (Fig. 6d), as expected (see e.g. [24]); the SCHC amplitude ratio T_{11}/T_{00} decreases with $|t|$ (Fig. 6c) .

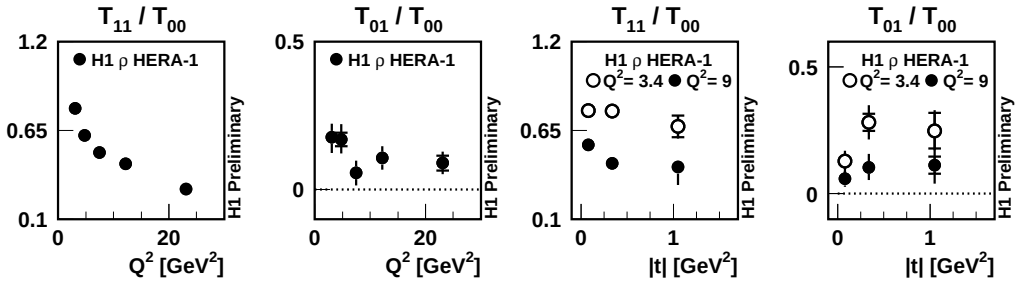

Fig. 6: Amplitude ratios T_{11}/T_{00} and T_{01}/T_{00} as a function of Q^2 and $|t|$ (for two bins in Q^2), for ρ electroproduction. The dotted lines represent the SCHC approximation.

Figure 7 presents measurements of the longitudinal to transverse cross ratio $R = \sigma_L/\sigma_T \simeq |T_{00}|^2/|T_{11}|^2$ (in the SCHC approximation). The behaviour $R \propto Q^2/M_V^2$ predicted for two-gluon exchange is qualitatively verified for all VM production, in fixed target and HERA ex-

[3] For detailed comparisons, modifications due to WF effects, as observed in VM electronic decay widths, may need to be taken into account.

periments. This is shown in Fig. 7-left, where R is plotted as a function of the scaled variable $Q^2 \cdot M_\rho^2/M_V^2$. However, the Q^2 dependence is tamed at large values of Q^2, a feature which is expected and relatively well described by pQCD based calculations, e.g. the GPD model [28], the k_t-unintegrated models [23, 24] or the dipole model [16].

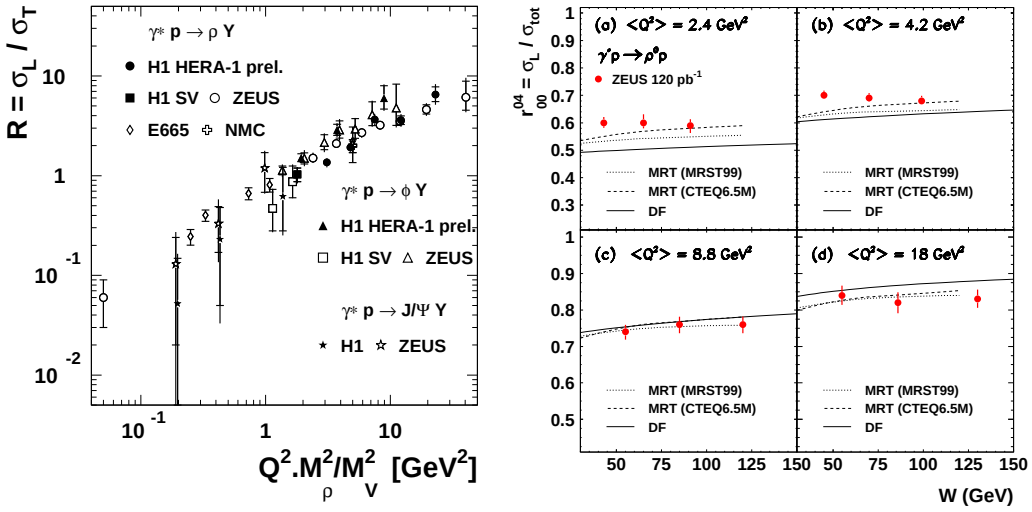

Fig. 7: Cross section ratio $R = \sigma_L/\sigma_T$ as a function of (left) the scaling variable $Q^2 \cdot M_\rho^2/M_V^2$ for different VM; (right) the centre of mass energy W in several Q^2 bins for ρ electroproduction, compared to model predictions.

The cross section ratio R for ρ electroproduction is also found to depend very significantly on the dipion mass $M_{\pi\pi}$ (not shown), in line with the Q^2/M_V^2 dependence if the relevant mass is the dipion mass rather than the nominal ρ resonance mass. Following the MRT model approach [23], this suggests a limited influence of the WF on VM production.

Figure 7-right shows that no strong dependence of R with W is observed. Since transverse amplitudes are expected to include significant contributions of large dipoles, with a soft energy dependence, this suggests that large dipoles are also present in longitudinal amplitudes, due to finite size effects, i.e. a smearing of z away from $z = 1/2$. On the other hand, in the domain $Q^2 \gtrsim 10 - 20$ GeV^2, no strong dependence of R with W is expected from models. It should also be noted that a significant phase difference is observed between the two dominant amplitudes, T_{00} and T_{11} [3]. This indicates a difference between the ratios of the real to imaginary parts of the forward amplitudes. Since these ratios are given by $\log 1/x$ derivatives of the amplitudes, the phase difference is an indication of different W dependences.

6 Large $|t|$; BFKL evolution

Large values of the momentum transfer $|t|$ provide a hard scale for diffractive processes in QCD, with the dominance of the proton dissociative channel for $|t| \gtrsim 1$ GeV^2. It should be noted that for large $|t|$ production, a hard scale is present at both ends of the exchanged gluon ladder. No

strong k_t ordering is thus expected, which is typical for BFKL evolutions for sufficiently high $|t|$ values. This is at variance with large Q^2 VM production at low $|t|$, where a large scale is present at the upper (photon) end of the ladder and a small scale at the proton end, implying that these processes are expected to be described by DGLAP evolutions, with strong k_t ordering along the ladder.

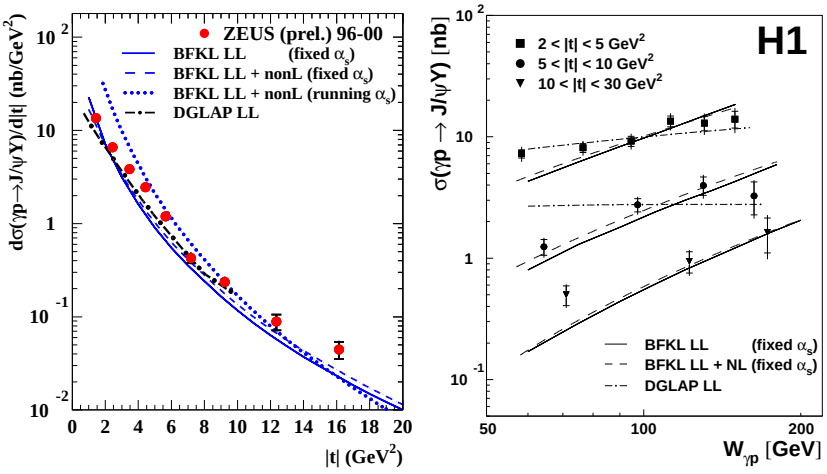

Fig. 8: t (left) and W (right) dependences of J/ψ production with $|t| > 2$ GeV^2, with comparisons to pQCD model predictions.

For $|t|$ larger than a few GeV^2, the t dependences of the cross sections follow power laws, both for ρ [4] and J/ψ [8] photoproduction. As shown by Fig. 8-left, they are well described by pQCD calculations based on the BFKL equations with fixed α_s [39]; predictions using the DGLAP evolution [40] also describe the J/ψ data for $|t| \lesssim m_\psi^2$. BFKL calculations describe the W evolution (Fig. 8-right), at variance with DGLAP, but do not describe well the spin density matrix elements. For ρ, ϕ and J/ψ photoproduction with $|t| \gtrsim 2$ GeV^2, the slope α' of the effective Regge trajectory tends to be slightly negative, but are compatible with 0.

7 Conclusions

In conclusion, studies of VM production and DVCS at HERA provide a rich and varied field for the understanding of QCD and the testing of perturbative calculations over a large kinematical domain, covering the transition from the non-perturbative to the perturbative domain. Whereas soft diffraction, similar to hadronic interactions, dominates light VM photoproduction, typical features of hard diffraction, in particular hard W dependences, show up with the developments of hard scales provided by Q^2, the quark mass or $|t|$. The size of the interaction is accessed through the t dependences. Calculations based on pQCD, notably using k_t-unintegrated gluon distributions and GPD approaches, and predictions based on models invoking universal dipole–proton cross sections describe the data relatively well. The measurement of spin density matrix

elements gives a detailed access to the polarisation amplitudes, which is also understood in QCD. Large $|t|$ VM production supports BFKL calculations.

Acknowledgements

It is a pleasure to thank the numerous colleagues from H1 and ZEUS who contributed to the extraction of the beautiful data presented here, and to thank the theorist teams whose efforts led to a continuous increase in the understanding of diffraction in terms of QCD, the theory of strong interactions. Special thanks are due to L. Motyka, T. Teubner and G. Watt for providing calculations used for the present review and to J.-R. Cudell and L. Favart for useful discussions and comments. It is also a pleasure to thank the organisors of the HERA-LHC Workshop for the lively discussions and the pleasant atmosphere of the workshop.

References

[1] H1 Coll., S. Aid et al., Nucl. Phys. **B 463**, 3 (1996);
ZEUS Coll., M. Derrick et al., Z. Phys. **C 73**, 253 (1997);
ZEUS Coll., J. Breitweg et al., Eur. Phys. J. **C 2**, 247 (1998);
H1 Coll., "A new Measurement of Exclusive ρ^0 Meson Photoproduction at HERA", XIV Int. Workshop on DIS, Tsukuba, Japan (2006);
ZEUS Coll., J. Breitweg et al., Eur. Phys. J. **C 6**, 603 (1999);
ZEUS Coll., J. Breitweg et al., Eur. Phys. J. **C 12**, 393 (2000);
H1 Coll., C. Adloff et al., Eur. Phys. J. **C 13**, 371 (2000);
H1 Coll., C. Adloff et al., Phys. Lett. **B 539**, 25 (2002).

[2] ZEUS Coll., S. Chekanov et al., PMC Phys. **A 1**, 6 (2007).

[3] H1 Coll., X. Janssen, "Diffractive ρ and ϕ production in DIS", XVI Int. Workshop on DIS, London, UK (2008);
H1 Coll., "Diffractive electroproduction of ρ and ϕ mesons at HERA", to be publ.

[4] ZEUS Coll., S. Chekanov et al., Eur. Phys. J. **C 26**, 389 (2003);
H1 Coll., A. Aktas et al., Phys. Lett. **B 638**, 422 (2006).

[5] ZEUS Coll., M. Derrick et al., Z. Phys. **C 73**, 73 (1996);
ZEUS Coll., J. Breitweg et al., Phys. Lett. **B 487**, 273 (2000).

[6] ZEUS Coll., M. Derrick et al., Phys. Lett. **B 377**, 259 (1996);
H1 Coll., C. Adloff et al., Phys. Lett. **B 483**, 360 (2000);
ZEUS Coll., S. Chekanov et al., Nucl. Phys. **B 718**, 3 (2005).

[7] ZEUS Coll., S. Chekanov et al., Eur. Phys. J. **C 24**, 345 (2002);
ZEUS Coll., S. Chekanov et al., Nucl. Phys. **B 695**, 3 (2004);
H1 Coll., A. Aktas et al., Eur. Phys. J. **C 46**, 585 (2006).

[8] H1 Coll., A. Aktas et al., Phys. Lett. **B 568**, 205 (2003);
ZEUS Coll., "Diffractive photoproduction of J/ψ mesons with large momentum transfer at HERA", subm. to XXXIII ICHEP, Moscow (2006).

[9] H1 Coll., C. Adloff et al., Phys. Lett. **B 541**, 251 (2002).

[10] ZEUS Coll., J. Breitweg et al., Phys. Lett. **B 437**, 432 (1998);
H1 Coll., C. Adloff et al., Phys. Lett. **B 483**, 23 (2000).

[11] ZEUS Coll., " Exclusive photoproduction of Υ mesons at HERA", submitted to the 2007 EPS Conference, Manchester (2007).

[12] ZEUS Coll., S. Chekanov et al., Phys. Lett. **B 573**, 46 (2003);
H1 Coll., A. Aktas et al., Eur. Phys. J. **C 44**, 1 (2005).

[13] H1 Coll., F. D. Aaron et al., Phys. Lett. **B 659**, 796 (2008).

[14] A.H. Mueller, Nucl. Phys. **B 335**, 115 (1990);
N.N. Nikolaev and B.G. Zakharov, Z. Phys. **C 49**, 607 (1991).

[15] J.R. Forshaw, R. Sandapen and G. Shaw, Phys. Rev. **D 69**, 094013 (2004).

[16] H. Kowalski, L. Motyka and G. Watt, Phys. Rev. **D 74**, 074016 (2006).

[17] H.G. Dosch and E. Ferreira, Eur. Phys. J. **C 51**, 83 (2007).

[18] K.J. Golec-Biernat and M. Wusthoff, Phys. Rev. **D 59**, 014017 (1999);
K.J. Golec-Biernat and M. Wusthoff, Phys. Rev. **D 60**, 114023 (1999);
S. Munier, A.M. Stasto and A.H. Mueller, Nucl. Phys. **B 603**, 427 (2001);
E. Iancu, K. Itakura and S. Munier, Phys. Lett. **B 590**, 199 (2004).

[19] L. Motyka, these proceedings.

[20] M.G. Ryskin, Z. Phys. **C 57**, 89 (1993);
J.S. Brodsky et al., Phys. Rev. **D 50**, 3134 (1994).

[21] L. Frankfurt, W. Koepf and M. Strikman, Phys. Rev. **D 54**, 3194 (1996).

[22] I.P. Ivanov, N.N. Nikolaev and A.A. Savin, Phys. Part. Nucl. **37**, 1 (2006).

[23] A.D. Martin, M.G. Ryskin and T. Teubner, Phys. Rev. **D 55**, 4329 (1997).

[24] D. Yu. Ivanov and R. Kirschner, Phys. Rev. **D 58**, 114026 (1998).

[25] T. Teubner, these proceedings.

[26] J. Collins, L. Frankfurt and M. Strikman, Phys. Rev. **D 56**, 2982 (1997).

[27] M. Diehl, Phys. Rep. **388**, 41 (2003);
A.V. Belitsky and A.V. Radyushkin, Phys. Rep. **418**, 1 (2005).

[28] S.V. Goloskokov and P. Kroll, Eur. Phys. J. **C 53**, 367 (2008).

[29] D. Yu. Ivanov, L. Szymanowski and G. Krasnikov, JETP Lett. **80**, 226 (2004);
D. Yu. Ivanov, A. Schafer, L. Szymanowski and G. Krasnikov, Eur. Phys. J. **C 34**, 297 (2004);
D. Yu. Ivanov, Blois Conference on Forward Physics and QCD, Hamburg (2007).

[30] A. Freund, Phys. Rev. **D 68**, 096006 (2003).

[31] L. Favart and M. V. T. Machado, Eur. Phys. J. **C 29**, 365 (2003).

[32] K. Kumericki, D. Mueller and K. Passek-Kumericki, Nucl. Phys. **B 794**, 244 (2008).

[33] A. Donnachie and P.V. Landshoff, Phys. Lett. **B 296**, 227 (1992);
J.-R. Cudell, K. Kang and S. Kim, Phys. Lett. **B 395**, 311 (1997).

[34] A. D. Martin, C. Nockles, M. G. Ryskin and T. Teubner, Phys. Lett. **B 662**, 252 (2008).

[35] G.A. Jaroszkiewicz and P.V. Landshoff, Phys. Rev. **D 10**, 170 (1974).

[36] S. J. Brodsky et al., JETP Lett. **70**, 155 (1999).

[37] J. Pumplin et al., JHEP **07**, 012 (2002).

[38] K. Schilling and G. Wolf, Nucl. Phys. **B 61**, 381 (1973).

[39] R. Enberg, L. Motyka and G. Poludniowski, Eur. Phys. J. **C 26**, 219 (2002).

[40] E. Gotsman, E. Levin, U. Maor and E. Naftali, Phys. Lett. **B 532**, 37 (2002).